

Applying Coherent and Incoherent Target Decomposition Techniques to Polarimetric SAR Data

Varsha Turkar
IIT Bombay

Center of Studies in Resource Engineering
IIT Bombay, Powai, Mumbai-400 076, India

Y.S.Rao
IIT Bombay

Center of Studies in Resource Engineering
IIT Bombay, Powai, Mumbai-400 076, India

ABSTRACT

Classification of polarimetric SAR images has become a very important topic after the availability of Polarimetric SAR images through different sensors like SIR-C, ALOS-PALSAR etc. In this paper we studied effect of different decomposition techniques on the classification accuracy for polarimetric SAR data. We applied different target decomposition techniques (both coherent and incoherent) on ALOS-PALSAR data over Sunderban, West Bengal district of India and later classified the data using various classification techniques. The same training areas are used for classification of decomposed images. A comparative study has indicated that Van Zyl decomposition gives better classification accuracy than other decomposition techniques. It is also observed that the H-A-Alpha decomposition along with the volume scattering F_v or V_v from the volume scattering component from Freeman and the VanZyl decomposition contributes a significant part to the improvement of classification. The accuracy for H-A-Alpha classified image is improved from 76.4% to 95.6% and to 96.2% after combining the volume scattering component from Freeman decomposition and Vanzyl decomposition respectively. The accuracy is further improved to 97% when the odd bounce component is combined along with volume scattering to H-A-Alpha for both the decompositions. It is observed that among the different classifiers applied, Maximum Likelihood Classifier gives highest accuracy.

Categories and Subject Descriptors

I.4.6 Image Processing and Computer Vision

General Terms

Algorithms, Measurements, Performance.

Keywords

Radar polarimetry, polarization, synthetic aperture radar, wetland, target decomposition, speckle, classification.

1. INTRODUCTION

Classification of polarimetric SAR images has become a very important topic after the availability of Polarimetric SAR images through ENVISAT ASAR, ALOS PALSAR, SIR-C and Radarsat-2. Classification is the task of assigning a set of given data elements to a given set of labels or classes such that the cost of assigning the data element to a class is minimum. Radar polarimetry is a well-established technique for classification of land use features. It has also become an

important and cost-effective tool for wetland investigation and researches. Wetlands are under pressure due to high demand for land development for housing and agriculture. Most of mangrove forests were cleared for settlements, agriculture and fire wood. It is important to manage the wetlands and conserve them for the benefit of the society, flora and fauna. Remote sensing is very useful tool to map the wetlands and classify them. Synthetic aperture radar technology is an advantage over optical remote sensing due to microwave penetration through vegetation and interaction with water under vegetation. The major steps of image classification may include determination of a suitable classification system, selection of training samples, image preprocessing and feature extraction, and selection of suitable classification approaches, post-classification processing and accuracy assessment. In this paper different target decomposition techniques are used before applying classification techniques. Same training sites are used for all the decompositions to do the comparative study of the results.

The objective of Target decomposition (TD) theory is to express the average scattering mechanism as the sum of independent elements to associate a physical mechanism with each component. There are two types of TD. One is Coherent (CTD) and other is Incoherent (ICTD).

CTD was developed to characterize completely polarized scattered waves for which fully polarimetric information is contained in the scattering matrix. The CTD can be used only to study coherent targets also known as point or pure targets. Man-made objects are the example of pure targets. Pauli, Krogager, Cameron are the Coherent type of decomposition. In this paper we have used Krogager decomposition. Krogager is also known as SDH decomposition because the scattering matrix can be represented as the combination of the response of sphere, diplane and helix. Helix scattering is a general scattering mechanism which appears in an urban area whereas disappears for almost all natural distributed scattering. It can distinguish man-made target from natural targets well but cannot divide one type of man-made target from another kind.

The scattering matrix is only able to characterize coherent or pure scatterers. However the matrix cannot characterize distributed scatterers (natural targets). ICTD was developed to characterize distributed scatterers. In this paper we have used Freeman, Van Zyl and Yamaguchi which are the types of ICTD. Freeman and Van Zyl has three types of scattering mechanisms namely volume, double bounce and surface or single bounce. Yamaguchi 4-component has one additional scattering mechanism that is helix. Helix scattering often appears in complex urban areas where as disappears in almost all natural distributed scenarios.

2. POLARIMETRIC DECOMPOSITION

The target decomposition was first introduced by Chandrasekhar (1960) [1] and later applied to polarized microwave by Huynen (1970) [2]. Coherent decomposition theorems use $[S]$ matrices. It considers a matrix $[S]$ as a linear combination of several other scatterers. A method for coherent target decomposition was presented by Krogager, 1988 [3]. His approach was based on the observation that any complex, symmetric scattering matrix can be decomposed into three components, as if the scattering were due to a sphere, a diplane and a right or left rotating helix. A three-component scattering model for polarimetric SAR data is proposed by Freeman and Durden (1998) [4]. Cloude et al. (1995, 1996) [5] have suggested the H-A-alpha target decomposition theorem. Van Zyl (1989) [6] describes the use of an imaging radar polarimetric data for unsupervised classification of scattering behavior by comparing the polarization properties of each pixel in an image to that of simple classes of scattering such as even number of reflections, odd number of reflections, and diffuse scattering. Coherent target decomposition methods can only be applied to coherent scattering. Generally, the scattered wave is partially polarized and the user might be interested in the extraction of geophysical parameters from an area that exhibits significant natural variability in the scattering properties (Van Zyl, 1992) [7]. For different target decomposition methods Alberga et al. (2004) [8] has applied Minimum Distance, Maximum Likelihood and Parallelepiped classifier. A four-component scattering model is proposed by Yamaguichi et al., 2005 [9] to decompose polarimetric synthetic aperture radar images. Circular polarization power is added as the fourth component to the three component scattering model which describes surface, double bounce, and volume scattering. This circular polarization term is added to take into account of the co-pol and the cross-pol correlations which generally appear in complex urban area scattering and disappear for natural distributed scatterer. Wang, et al (2009)[10] proposed a method of unsupervised classification of polarimetric SAR data based on image clustering and H/A/ α decomposition. Fully polarimetric L band data collected by ALOS PALSAR system was used in this paper. The relation between physical structure and polarimetric signal properties is studied explicitly using polarimetric decomposition [16]. The 'H/A/ α ' decomposition theorem is the basis for the design of the proposed processing scheme for polarimetric SAR images. An improved land-cover classification based on this indicates the scattering properties of target classes very well and hence can be used to produce a much more improved classification result. The volume scattering F_v from the Freeman decomposition contributes a significant part to the improvement of classification. A comparison of polarimetric target decomposition methods is proposed by Zhang et al. (2008) [11]. Results show that among many target decomposition algorithms, the coherent and incoherent formulations are quite comparable in distinguishing natural targets and man-made buildings. Pauli decomposition, Cameron decomposition and Freeman decomposition are suitable for the detection of natural targets. On the other hand, SDH decomposition, OEC decomposition, and Four-component model, in particular, are very useful for man-made target extraction. The Touzi decomposition is investigated for wetland characterization [12]. A target scattering decomposition was investigated by Touzi et al. (2009) [13], for wetland classification. The Touzi decomposition, which permits a roll-invariant target scattering decomposition, leads to the characterization of wetland classes in terms of unique target parameters. Ballester-Berman et al. (2010)

[14] proposed a procedure for exporting the Freeman–Durden PolSAR TD concept to PolInSAR data. The formulation of the Freeman–Durden decomposition has been adapted to PolInSAR in order to jointly retrieve not only the magnitude but also the interferometric phases (related to the vertical locations) of the direct (odd-bounce), double-bounce, and volume scattering mechanisms.

3. TEST SITES AND DATA SOURCES

ALOS PALSAR data in fully polarimetric mode was acquired over Sunderban, West Bengal district of India on May 21, 2007. Close to the area covering Gangetic plains with agriculture is also acquired by ALOS PALSAR on May 21, 2008.

Sunderban is a part of the world's largest mangrove forest. It is located in southern West Bengal. Lothian Island Wildlife Sanctuary lies south of Sunderbans in South 24 Parganas District, West Bengal. This 2,585-sq km park is the world's largest mangrove forest. Named after the Sundari trees, once found in large quantities here, the park features an extremely diverse array of vegetation and plant life, as well as houses an astounding variety of wildlife. It is the home of the endangered Royal Bengal tiger. In addition to the tigers, the sanctuary is also home to other wild and marine life, including wild boars, macaques, jungle cats, chitals, monkeys, Olive Ridley turtles, dolphins, sea snakes, king cobras and estuarine crocodiles to name a few.

4. DATA PROCESSING

The target decomposition techniques are applied with the help of PolSARPro software on ALOS-PALSAR Sunderban area. The software creates files one file for each scattering mechanism for example for Freeman decomposition it creates three files namely Freeman_dbl.bin, Freeman_vol.bin, Freeman_odd.bin for double bounce, volume scattering and odd bounce scattering respectively. These three files are separately processed using ENVI software. Further the three files are combined to form one file: Freeman_dbl_vol_odd. This file is further processed by different classifiers namely Minimum Distance Classifier (MDC), Maximum Likelihood Classifier (MLC), Parallelepiped and Mahalanobis. The chosen algorithms implement quite general image classification methods and are not specifically intended for SAR data; hence they are not the optimal tools for analyzing them. Since these classifiers are the simpler approaches and are available to wide array of potential users, it would be the method of choice. The same procedure is done for all the decompositions.

5. RESULTS

After applying the decompositions, different classification techniques are applied using ENVI. Table 1 show the classification accuracy of various features for three separate components of Freeman and Van Zyl decomposition namely Double, Volume and Odd or Single bounce. From figures 1, 2 and the table no 1 it is clearly seen that Van Zyl decomposition gives better accuracy than Freeman decomposition. For double bounce scattering Van Zyl gives 20% more accuracy than that of Freeman. From the results of both the decompositions, it is clearly seen that wetland gives odd bounce scattering and mangrove gives volume scattering. Figure 1 and 2 shows the classified images using Freeman and Van Zyl decomposition respectively. Figure 1 (a) and figure 2 (a) are the decomposed images before classification. In this red color shows double bounce, green shows volume scattering and blue shows odd bounce scattering. Figure 1 and 2 (b)-(e) shows the classified images after applying different classifiers namely Minimum Distance (MDC), Mahalanobis,

Parallelepiped and Maximum Likelihood (MLC) respectively. Table 2 (a)-(e) shows confusion matrices for ALOS/PALSAR Sunderban area computed after applying Minimum distance classifier for different decompositions. Table 3 gives comparison of classification accuracies for different decompositions for different classifiers.

After comparing the results with other decomposition techniques like Freeman, Krogager, Yamaguchi-3 and -4 components it is

found that Van Zyl decomposition gives the best results than all these decomposition techniques.

The classification accuracy for mangrove is highest (93.55%) in case of Van Zyl which is much more than all other decomposition. The results are verified by using different classifiers like Mahalanobis, Parallelepiped, MDC and MLC. The result for ML classifier is the best among all the classifiers.

Table 1: Classification accuracy for double, volume and odd bounce scattering. (a) Freeman (b) Van Zyl

	Double	Volume	Odd
Accuracy	52.80%	61.94%	41.72%
Mangrove	12.83	81.07	26.62
Water	86.79	34.59	28.21
Agri-bare	21.2	98.08	83.17
Veg+village	57.3	83.02	25.48
Wetland	1.42	55.38	92.02

(a)

	Double	Volume	Odd
Accuracy	71.51%	63.23%	46.14%
Mangrove	74	90.05	70.94
Water	79.83	37.39	34.7
Agri-bare	71.38	85.28	47.26
Veg+village	63.46	78.97	26.02
Wetland	13.78	79.59	99.94

(b)

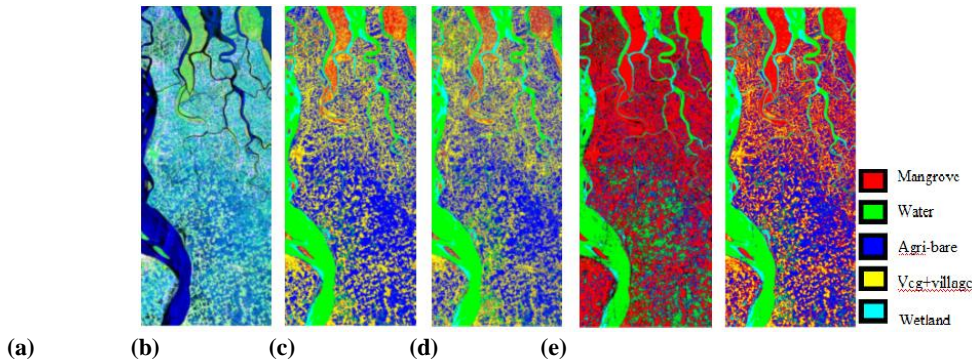


Figure 1: Classified images for Freeman decomposition (a) Freeman_dbl_vol_odd_db (before classification) Red = double bounce, Green = volume scattering, Blue = odd or single bounce (b) Minimum distance classified image (c) Mahalanobis classified image (d) Parallelepiped classified image (e) Maximum likelihood classified image

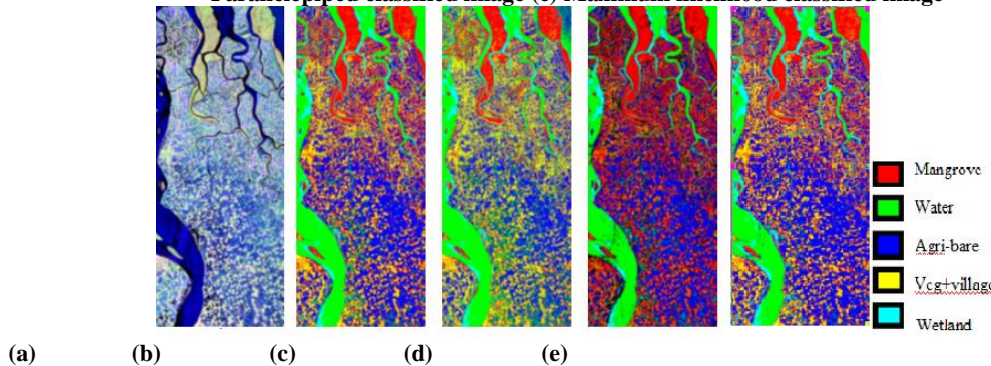


Figure 2: Classified images for Van Zyl decomposition (a) Van Zyl3_dbl_vol_odd_db (before classification (b) Minimum distance classified image (c) Mahalanobis classified image (d) Parallelepiped classified image (e) Maximum likelihood classified image

Table 2: Confusion matrices for ALOS-PALSAR Sunderban area

Class	Mangrove	Water	Agri-bare	Veg+Village	Wetland	Total
Mangrove	64.98	0	0	11.39	0.26	12.88
Water	0	96.17	1.13	0	0.64	44.07
Agri-bare	0.59	3.81	98.85	0.24	0.07	20.82
Veg+Village	34.43	0	0.02	88.37	0	16.66
Wetland	0	0.02	0	0	99.03	5.56

(a) Freeman

Class	Mangrove	Water	Agri-bare	Veg+Village	Wetland	Total
Mangrove	93.55	0	0.15	8.37	0.06	17.6
Water	0	99.9	2.49	0	0.58	46.03
Agri-bare	0.06	0.06	97.36	0.06	0.26	18.72
Veg+Village	6.38	0	0	91.57	0	12.07
Wetland	0	0.04	0	0	99.1	5.58

(b) Van Zyl

Class	Mangrove	Water	Agri-bare	Veg+Village	Wetland	Total
Mangrove	40	9.16	4.65	4.32	1.74	12.76
Water	13.16	54.45	28.19	9.4	1.55	33.75
Agri-bare	10.48	33.28	35.03	13.75	0.32	25.39
Veg+Village	36.35	1.21	32.01	72.5	0	21.79
Wetland	0.02	1.89	0.11	0.03	96.39	6.3

(c) Krogager

Class	Mangrove	Water	Agri-bare	Veg+Village	Wetland	Total
Mangrove	56.52	0	1.17	19.16	0.06	12.53
Water	0	91.15	11.76	0.03	3.03	43.96
Agri-bare	7.55	7.86	86.07	5.44	0.13	22.08
Veg+Village	33.69	0	0.94	74.86	0	15.09
Wetland	2.24	0.98	0.06	0.51	96.78	6.35

(d) Yamaguchi_3

Class	Mangrove	Water	Agri-bare	Veg+Village	Wetland	Total
Mangrove	9.81	0	0	8.16	3.86	2.93
Water	5.57	86.85	23.89	2.48	49.26	48.2
Agri-bare	66.76	9.8	69.96	71.41	0.26	38.25
Veg+Village	9.04	3.35	6.14	13.12	3.54	6.07
Wetland	8.83	0	0	4.84	43.08	4.56

(e) Yamaguchi_4

Table 3: Classification accuracies for different decompositions for different classifier

Classifier	Freeman	Van Zyl3	Krogager	Yamaguchi3	Yamaguchi4
Minimum Distance	90.39%	97.25%	52.68%	82.41%	48.51%
Mahalanobis	84.53%	85.64%	72.34%	77.14%	60.87%
Parallelepiped	74.50%	89.27%	34.16%	69.22%	46.91%
Maximum Likelihood	96.83%	97.84%	80.98%	85.44%	71.52%

As discussed before ICTD is giving better accuracy for this type of data set since it has more natural or distributed scatterers than pure scatterers. Yamaguchi 4 gives poor classification accuracy. The 4th helix scattering component Pc in Yamaguchi 4 decomposition becomes minor contribution for the natural distributed target area [15].

The H-A-Alpha decomposition is applied on the polarimetric Sunderban data set. The three components entropy, anisotropy and alpha are combined to form one binary file "h_a_alpha.bin". Maximum Likelihood classification technique is applied on this

file using ENVI. Wang, et.al (2009) [10] used volume scattering (Fv) component to further refinement of the classification due to its ability to reflect the mechanism of targets. High value of Fv suggests strong volume scattering and lower value of Fv often indicates strong surface scattering. Figure 3 shows four parameters entropy, anisotropy, alpha and Fv images which are combined to get better classification results. Figure 4 shows the H-A-Alpha, H-A-Alpha with Fv and H-A-Alpha with Vv classified images and the corresponding confusion matrix is given in table no 3. The classification accuracy increases from

76% to 95% after combining the volume scattering component with H-A-Alpha.

Figure 5 (a) and (b) shows the classified images for H-A-Alpha with volume and odd bounce scattering component.

The classification accuracy is given by the confusion matrix shown in table no. 4. The Accuracy is further increased from

95% to 97% after adding the odd bounce component. When all the three components (volume, odd and double bounce) are combined with H-A-Alpha it is observed that the accuracy is further increased to 98%.

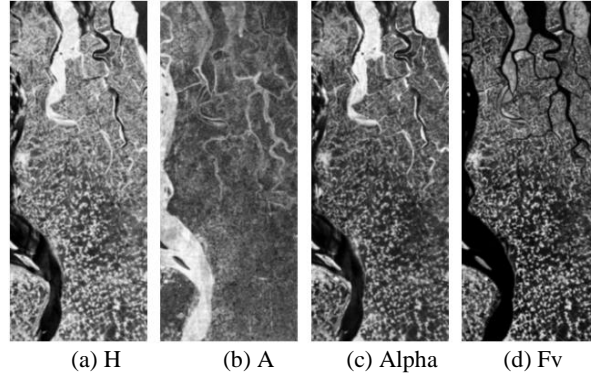
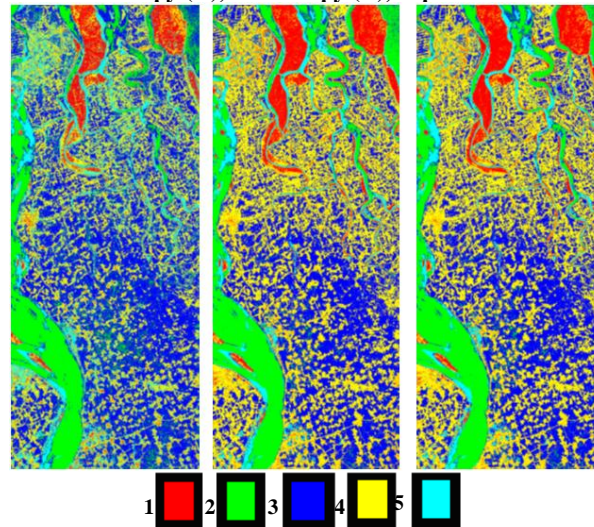


Figure 3: Parameters Entropy (H), Anisotropy (A), Alpha and Volume scattering (Fv)



1: Mangrove, 2: Water, 3: Agri-bare, 4: Veg+Village, 5: Wetland

Figure 4: Maximum likelihood classified images (a) H-A-Alpha (b) H-A-Alpha+Fv (c) H-A-Alpha+Vv

Table 3: Confusion matrix (Fv: Freeman volume scattering, Vv: VanZyl volume scattering)

Class	Mangrove	Water	Agri-bare	Veg+Village	Wetland	Total
Mangrove	79.73	0	0	29.74	7.92	18.12
Water	0	76.03	17.05	0.03	0	37.91
Agri-bare	0.06	23.97	82.87	0.6	0.45	26.92
Veg+Village	14.95	0	0.02	60.14	9.4	10.37
Wetland	5.26	0	0.06	9.49	82.23	6.69
Total	100	100	100	100	100	100

(a) Overall accuracy= 76.4438% Kappa =0.6762 for classified H-A-Alpha

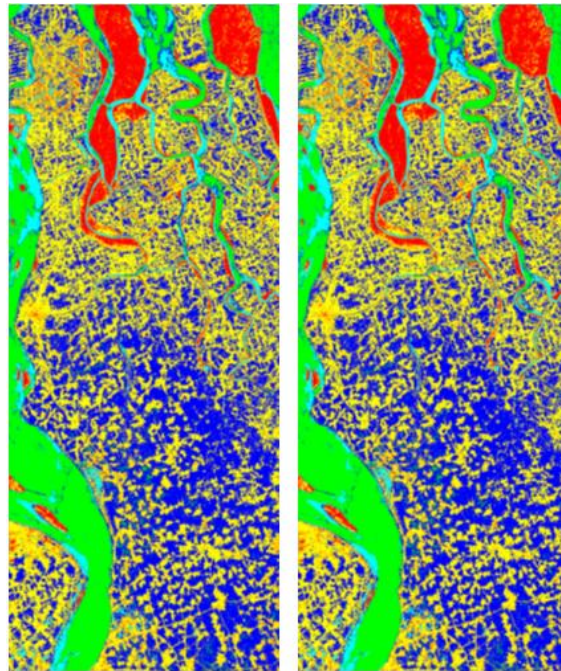
Class	Mangrove	Water	Agri-bare	Veg+Village	Wetland	Total
Mangrove	93.39	0	0	9.13	0.77	17.67
Water	0	96.16	1.34	0	0.06	44.07
Agri-bare	0	3.84	98.53	0.03	0.39	20.66
Veg+Village	6.61	0	0.13	90.84	0.26	12.07

Wetland	0	0	0	0	98.52	5.53
Total	100	100	100	100	100	100

(b) Overall accuracy =95.62% Kappa = 0.9384 for classified H-A-Alpha+ Fv

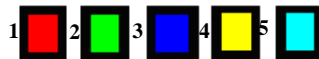
Class	Mangrove	Water	Agri-bare	Veg+Village	Wetland	Total
Mangrove	95.33	0	0	6.17	0.64	17.65
Water	0	96.13	1.66	0	0.06	44.12
Agri-bare	0	3.87	98.21	0.03	0.39	20.61
Veg+Village	4.67	0	0.13	93.8	0.32	12.08
Wetland	0	0	0	0	98.58	5.53
Total	100	100	100	100	100	100

(c) Overall accuracy= 96.25% Kappa= 0.9472 for classified H-A-Alpha+ Vv



(a)

(b)



1: Mangrove, 2: Water, 3: Agri-bare, 4: Veg+Village, 5: Wetland

Figure 5: Maximum likelihood classified images (a) H-A-Alpha+Fv+Fo (c) H-A-Alpha+Vv+Vo

Table 4: Confusion matrix (Fv: Freeman volume scattering, Fo: Freeman odd bounce scattering, Vv: VanZyl volume scattering, Vo: Vanzyl odd bounce scattering)

Class	Mangrove	Water	Agri-bare	Veg+Village	Wetland	Total
Mangrove	95.64	0	0	4.62	0.58	17.52
Water	0	98.41	0.96	0	0.19	45.04
Agri-bare	0	1.59	98.94	0.03	0.19	19.7
Vegetation	4.36	0	0.09	95.35	0.26	12.2
Wetland	0	0	0	0	98.78	5.54
Total	100	100	100	100	100	100

(a) Overall accuracy =97.68% Kappa= 0.9672 for classified H-A-Alpha+Fv+Fo

Class	Mangrove	Water	Agri-bare	Veg+Village	Wetland	Total
Mangrove	96.02	0	0	3.54	0.52	17.46
Water	0	98.37	1	0	0.13	45.02
Agri-bare	0	1.63	98.91	0.03	0.26	19.72
Vegetation	3.98	0	0.09	96.43	0.26	12.26
Wetland	0	0	0	0	98.84	5.54
Total	100	100	100	100	100	100

(b) Overall accuracy =97.85% Kappa= 0.9697 for classified H-A-Alpha+Vv+Vo

6. CONCLUSION

Different target decomposition techniques have been applied on ALOS-PALSAR Sunderban data set for finding classification accuracy. It is observed that among Freeman, Van Zyl, Krogager, Yamaguchi 3-components and 4- components decomposition Van Zyl gives the best results. The Van Zyl decomposition gives better classification accuracy for mangroves (93.55%) while Freeman decomposition gives almost 30% less than Van Zyl. The overall classification accuracy obtained by Van Zyl is 97.8%. ICTD is giving better accuracy for this type of data set since it has more natural or distributed scatterers than pure scatterers. It is also observed that the H-A-Alpha decomposition along with the volume scattering Fv or Vv from the volume scattering component from Freeman and the VanZyl decomposition contributes a significant part to the improvement of classification. The accuracy for H-A-Alpha classified image is improved from 76.4% to 95.6% and to 96.2% after combining the volume scattering component from Freeman decomposition and Vanzyl decomposition respectively. The accuracy is further improved to 97% when the odd bounce component is combined along with volume scattering to H-A-Alpha for both the decompositions.

7. ACKNOWLEDGEMENT

ALOS-PALSAR data were obtained through announcement opportunity of JAXA, Japan under project no. 381

8. REFERENCES

- [1] Chandrasekhar, S. 1960. Radiative transfer. Dover, New York
- [2] Huynen, J. R.(1970). "Phenomenological theory of radar targets", PhD thesis, Technical University of Delft, the Netherlands.
- [3] Krogager, E. (1988). "Decomposition of the Sinclair matrix into fundamental components with applications to high resolution radar target imaging", Proceedings of the NATO-ARW, Bad Windsheim, West Germany, pp.18-24.
- [4] Freeman, A., Durden, S.L.(1998). "A Three-Component Scattering Model for Polarimetric SAR Data" IEEE TGRS, vol. 36, no. 3.
- [5] Cloude, S.R., Pottier, E. (1996). "A review of target decomposition theorems in radar polarimetry", IEEE Transactions on Geoscience and Remote Sensing, Vol. 34, No. 2, pp. 498–518.
- [6] Van Zyl, J.J., (1989). "Unsupervised Classification of Scattering Behavior Using Radar Polarimetry Data", IEEE Transactions on Geoscience and Remote Sensing, Vol 27, No 1, pp. 37–45.
- [7] Van Zyl, J.J., (1992). "Application of Cloude's target decomposition theorem to polarimetric imaging radar data", In Radar polarimetry. Edited by H. Mott and W.M.
- [8] Alberga, V.; Krogager, E.; Chandra, M.; Wanielik, G., (2004). "Potential of coherent decompositions in SAR polarimetry and interferometry", International Geoscience and Remote Sensing Symposium.
- [9] Yamaguchi, Y., Moriyama, T., Ishido, M., Yamada, H., (2005). "Four-component scattering model for polarimetric SAR image decomposition," IEEE TGRS, vol.43, no. 8.
- [10] Wang, L., Zhang, Y., Lu, X., Wang, P. (2009). "Unsupervised Classification of Polarimetric SAR Data Using Image Clustering and H/A/α Decomposition" Proceedings of the ISPRS, Vol.XXXVIII-7/C4, pp. 268-271.
- [11] Zhang, L., Zhang, J., Zou, B. and Zhang, Ye.,(2008). "Comparison of Methods for Target Detection and Applications Using Polarimetric SAR Image", Piers online, Vol. 4, No. 1.
- [12] Touzi, R., Deschamps, A. and Rother, G., (2008). "Scattering type phase for wetland classification using C-band polarimetric SAR", IGARSS.
- [13] Touzi, R., Deschamps, A. and Rother, G.,(2009). "Phase of Target Scattering for Wetland Characterization Using Polarimetric C-Band SAR", IEEE Transactions on Geoscience and Remote Sensing, Vol. 47, No. 9, pp. 3241-3261.
- [14] Berman, D.B., Lopez-Sanchez, J., Juan, M. (2010). "Applying the Freeman–Durden Decomposition Concept to Polarimetric SAR Interferometry", IEEE Transactions on Geoscience and Remote Sensing, Vol. 48, NO. 1, pp. 466-479.
- [15] Sato, R., Yamaguchi and Yamada, H. (2009). "Polarimetric scattering feature estimation for accurate vegetation area classification", Proc. IGARSS, Vol. 2, pp. 888-891.
- [16] Turkar, V., Rao, Y.S. (2011). "Effect of different decomposition techniques on classification accuracy for polarimetric SAR data", Proc. ICTSM 2011, CCIS 145, pp. 138–145.